



저작자표시-비영리-변경금지 2.0 대한민국

이용자는 아래의 조건을 따르는 경우에 한하여 자유롭게

- 이 저작물을 복제, 배포, 전송, 전시, 공연 및 방송할 수 있습니다.

다음과 같은 조건을 따라야 합니다:



저작자표시. 귀하는 원저작자를 표시하여야 합니다.



비영리. 귀하는 이 저작물을 영리 목적으로 이용할 수 없습니다.



변경금지. 귀하는 이 저작물을 개작, 변형 또는 가공할 수 없습니다.

- 귀하는, 이 저작물의 재이용이나 배포의 경우, 이 저작물에 적용된 이용허락조건을 명확하게 나타내어야 합니다.
- 저작권자로부터 별도의 허가를 받으면 이러한 조건들은 적용되지 않습니다.

저작권법에 따른 이용자의 권리는 위의 내용에 의하여 영향을 받지 않습니다.

이것은 [이용허락규약\(Legal Code\)](#)을 이해하기 쉽게 요약한 것입니다.

[Disclaimer](#)

Verification of Recombinant *Mycobacterium smegmatis* in bladder cancer mice model and discovery of diagnostic markers through the application of bladder cancer clinical data

Dongwook Song

**The Graduate School
Yonsei University
Department of Intergrative Medicine**

Verification of Recombinant *Mycobacterium smegmatis* in bladder cancer mice model and discovery of diagnostic markers through the application of bladder cancer clinical data

**A Master's Thesis submitted to the Department
of Department of Integrative Medicine
and the Graduate School of Yonsei University
in partial fulfillment of the
requirements for the degree of
Master of Health Science**

Dongwook Song

June 2024

**This certifies that the Masters Thesis
of Dongwook Song is approved.**

Thesis Supervisor [Young Deuk Choi]

Thesis Committee Member [Hyunho Han]

Thesis Committee Member [Yong Seung Lee]

**The Graduate School
Yonsei University
June 2024**

ACKNOWLEDGEMENTS

Firstly, I would like to extend my deepest gratitude to my advisor, Prof. Young Deuk Choi for his continuous support throughout my master's program, which enabled me to graduate successfully. His unchanging support from the beginning to the end was instrumental in my graduation. I also want to express my sincere appreciation to my co-advisor, Prof. Hyun ho Han. His guidance helped me when I was lacking direction at the start of my research and facilitated my understanding of the topic of this thesis. Without his assistance, I could not have reached this outcome. Besides my advisors, I would like to thank Prof. Yong Seung Lee, a member of my thesis committee. Without their feedback and encouragement, I would not have been able to successfully conclude my research. Furthermore, I am grateful to Dr. Baek Gil Kim and Dr. Yeonsue Jang for assisting me with various perspectives and methods, steering my thesis in the right direction. Finally, I want to express my sincerely thanks to my lovely family for their unchanging belief in me and their continuous support throughout this journey.

TABLE OF CONTENTS

LIST OF FIGURES	iii
LIST OF TABLES	iii
ABSTRACT (IN ENGLISH)	iv
1. INTRODUCTION	1
2. MATERIALS AND METHODS	3
2.1. Mice	3
2.2. Tumor cell culture	3
2.3. Tumor implantation and size measurement	3
2.4. rSmeg-MIF-IL7 strain culture	3
2.5. Immunization in mice with rSmeg-MIF-IL7 strain	4
2.6. The mRNA sequencing analysis	4
2.7. Enrichment analysis of DEGs	5
2.8. Calculation of cell fraction abundance of immune cells	5
2.9. Kaplan–Meier plotter database analysis	5
2.10. cBioPortal for cancer genomics database analysis	5
2.11. RNA isolation and quantitative real-time-PCR (qPCR)	6
2.12. Statistical analysis	6

3. RESULTS	7
3.1. rSmeg-MIF-IL7 vaccine inhibited tumor progression in a syngeneic mouse model of bladder cancer	7
3.2. DEGs between two groups in primary tumor cells are associated with immune response pathway and negative regulation of angiogenesis	9
3.3. CD8+, CD4+ memory T cells activated, abundance in rSmeg-MIF-IL7 group.....	12
3.4. Prognostic diagnostic markers screening in TCGA Bladder Urothelial Carcinoma study.....	13
3.5. Differences in Neoplasm stage and grade based on gene expression levels in patients.....	16
3.6. Validation of diagnostic marker expression at both mRNA and protein level in bladder-cancer.....	18
4. DISCUSSION	20
5. CONCLUSION	22
REFERENCES	23
ABSTRACT (IN KOREAN)	26

LIST OF FIGURES

Figure 1. Schematic outline diagram of overall rSmeg-MIF-IL7 immunization process and diagnosis markers analysis process	2
Figure 2. Tumor volume measurements and survival analysis of rSmeg-MIF-IL7 immunization test in the MBT-2 syngeneic subcutaneous tumor mice	8
Figure 3. Gene expression overview in rSmeg-MIF-IL7 treated group compared to the control-group	10
Figure 4. Immune cells infiltration generated using CIBERSORTx	12
Figure 5. Diagnosis markers selection by using TCGA bladder cancer (TCGA-BLCA) clinic data set and KMplotter	14
Figure 6. Summary of neoplasm stage and histologic grade based on gene expression in bladder cancer patients	17
Figure 7. Validation of Diagnosis markers by QRT-PCR results and Immunohistochemistry staining images	19

LIST OF TABLES

Table 1. Representative significantly enriched pathways of top20 gene ontology biological process and related DEGs	11
--	----

ABSTRACT (IN ENGLISH)

Verification of Recombinant *M. smegmatis* in Bladder Cancer Mice Model and Discovery of diagnostic markers through the application of bladder cancer clinical data

BCG (*Bacillus Calmette–Guérin*) therapy, a treatment for bladder tumor, is known as the most effective and only treatment that can inhibit the progression from high-risk NMIBC to MIBC after TURBT. However, approximately 30-45% of NMIBC patients show no response, and about 20% experience side effects. Moreover, BCG production faces a global supply shortage due to the slow growth rate of the tuberculosis bacterium and strict manufacturing processes. Previous studies have suggested the potential of the rSmeg-MIF-IL7 vaccine as an alternative to BCG for anti-tumor immunotherapy. Here, we first created a mouse bladder cancer model and administered the rSmeg-MIF-IL7 vaccine, confirming its anti-tumor effects. Additionally, bioinformatics analysis revealed immune infiltration of CD8⁺ and CD4⁺ memory T cells within tumor samples from the rSmeg-MIF-IL7 group. To further investigate the clinical therapeutic potential, we conducted an association analysis of our gene expression data with the TCGA dataset. As a result, we identified 8 genes, including CCL15 and SIGLEC6, as diagnostic markers capable of distinguishing patient groups suitable for rSmeg-MIF-IL7 vaccine therapy based on gene expression related to survival and malignancy. In conclusion, we demonstrated the anti-tumor effects of rSmeg-MIF-IL7 in a mouse bladder cancer model and confirmed its potential for clinical application.

Key words: bladder cancer, rSmeg-MIF-IL7, BCG, immune infiltration, CCL15, SIGLEC6

1. INTRODUCTION

Bacillus Calmette–Guérin (BCG) therapy is recognized as the most effective therapy for suppressing the progression to muscle-invasive bladder cancer (MIBC) following transurethral resection of bladder tumor (TURBT) for high-risk non-muscle-invasive bladder cancer (NMIBC) [1], [2], [3]. However, approximately 30-45% of NMIBC patients do not respond to BCG therapy, leading to disease progression [4]. Moreover, about 20% of patients may experience side effects such as bladder inflammation, irritability, hematuria, and BCG sepsis, potentially leading to treatment discontinuation [5]. Additionally, BCG production faces global shortages due to the slow growth rate of *Mycobacterium tuberculosis* and stringent manufacturing processes. Although several alternatives like Gemcitabine and Docetaxel combination to BCG have been explored, none have demonstrated superior efficacy, particularly in terms of tumor differentiation [6].

Cancer immunotherapy aims to treat cancer by enhancing the immune system's capabilities. Specifically, T cell-based immunotherapy has emerged as a promising strategy against various types of cancer [7]. Presented as an alternative to BCG, rSmeg-MIF-IL7 tumor immunotherapy is a recombinant *Mycobacterium smegmatis* vaccine that delivers fusion proteins of human Macrophage Migration Inhibitory Factor (MIF) and IL-7 [8], [9]. *Mycobacterium smegmatis*, a rapidly growing mycobacterium, induces dendritic cell maturation more effectively than BCG and can stimulate CD8⁺ T cell immune responses, thereby offering a benefit in inducing CTL responses [10]. The antigenic human MIF, known to be expressed in solid tumors and associated with a malignant prognosis, induces anti-MIF antibody responses to promote inhibition within the body [11]. Interleukin 7 (IL-7) increases the number of memory CD8⁺ T cells, enhancing anti-tumor immunity and suppressing tumors [12]. While previous studies have confirmed the tumor-suppressive effects of rSmeg-MIF-IL7 in mouse models of various cancers, its effectiveness in bladder cancer models has yet to be demonstrated, and evaluation based on clinical data remains pending [10].

Therefore, in this study, we established a syngeneic subcutaneous bladder cancer model using MBT-2 (Murine Bladder Tumor-2) cells derived from CH3/He mice. We demonstrated that immunotherapy with rSmeg-MIF-IL7 exhibited significant anti-cancer effects by restoring CTL responses through the regulation of various genes in this bladder cancer model. Additionally, through gene analysis and correlation analysis with The Cancer Genome Atlas (TCGA) dataset of

bladder cancer patients, our aim is to identify clinically significant diagnostic markers of rSmeg-MIF-IL7 therapy and propose suitable bladder cancer patient groups for clinical application using these diagnostic markers (Figure 1).

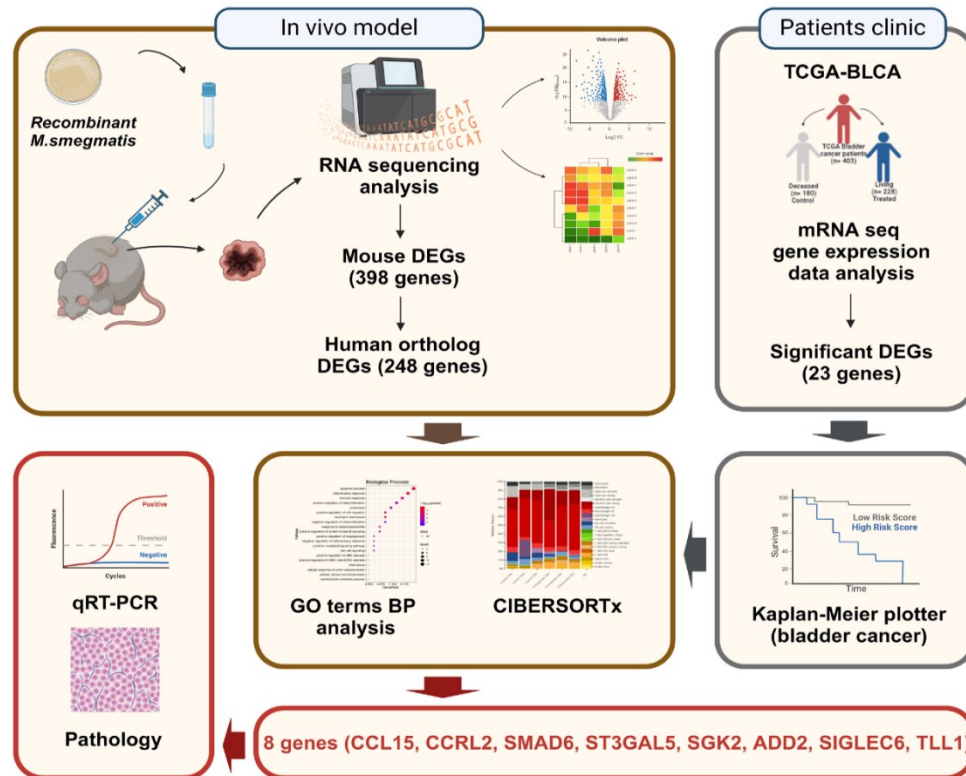


Figure 1. Schematic outline diagram of overall rSmeg-MIF-IL7 immunization process and diagnosis markers analysis process

2. MATERIALS AND METHODS

2.1. Mice

Female CH3/He mice were acquired from Orient-Bio (Seoul, Korea) and were employed for experiments at 8 weeks of age. All animal experiments were approved by the Institutional Animal Care Use Committee (IACUC; approval no. 2021-0079) of the Department of Laboratory Animal Resources, Yonsei Biomedical Research Institute, Yonsei University College of Medicine, Republic of Korea.

2.2. Tumor cell culture

MBT-2, a murine bladder tumor cell line, represents mouse bladder transitional cell carcinoma. MBT-2 cells are derived from N-{4-(5-nitro-2-furyl)-2-thiazolyl} formamide (FANFT) induced C3H/He mouse. MBT2 cells (Cat No. IFO50041) were purchased from the JCRB Cell Bank (Tokyo, Japanese). The cells were cultured in MEM (Gibco) with 10% heat-inactivated fetal bovine serum, 2mM Glutamine, 25 mM HEPES, and 1% penicillin-streptomycin at 37°C in a 5% CO₂ incubator. Cultures were split into 100Ø culture dish (SPL) and whole cell extracts were collected upon reaching 70%-80% confluence by employing trypsin/EDTA (0.25%, 0.9 mM EDTA) (Gibco)..

2.3. Tumor Implantation and size measurement

The dorsal area of ether inhalation-anesthetized mice was shaved using hair trimmer. Mice were subcutaneously inoculated with 2.0×10^6 MBT-2 cells/ml. We used 10-12 mice per experiment, and the experiment was conducted a total of 3 times. Tumor size was measured from 6 day post inoculation and once every 2 or 3 days with electronic calipers. The total volume was calculated using the following formula: $\{(\text{short diameter})^2 \times \text{long diameter}\} / 2$ (mm³). Animals were euthanized based on either tumor volume {threshold 1500 (mm³)} in accord with IACUC guidelines.

2.4. rSmeg-MIF-IL7 strain culture

The rSmeg-MIF-IL7 strain was constructed by Department of Microbiology and Immunology, College of Medicine, Seoul National University, Seoul and CLIPS Bnc Co.. the strain was obtained

through material transfer from Seoul National University Industry Foundation-Yonsei University Health System. Colonies of the rSmeg-MIF-IL7 strain were chosen on 7H10 medium (Difco Laboratories, Detroit, MI, USA), supplemented with 100µg/ml kanamycin and 10% OACD (oleic acid-albumin-dextrose-catalase). The chosen colonies were grown in 7H9 broth medium (Difco Laboratories, Detroit, MI, USA) supplemented with 0.5% glycerol, 0.05% Tween-80, 10% ADC, and kanamycin for about 3-5 days. The cultured rSmeg-MIF-IL7 was prepared to attain an optical density (OD) at 600 nm within the range of 0.5-0.8.

2.5. Immunization in mice with rSmeg-MIF-IL7 strain

The cultured rSmeg-MIF-IL7 strain was prepared by mixing it with PBS after centrifugation. The injection volume was 100µl in rSmeg-MIF-IL7 group. Mice were treated by intraperitoneal injection using a 31G 8mm insulin syringe every once every two days.

2.6. The mRNA sequencing analysis

Total RNA was extracted from each of the three samples belonging to both the rSmeg-MIF-IL7 and control groups. Subsequently, RNA-seq libraries were constructed using the Illumina TruSeq Stranded Total RNA Sample Prep kit (Catalog #RS-122-2103; Illumina, San Diego, CA, USA). Quantification of the libraries was conducted through qPCR, following the qPCR Quantification Protocol Guide, with results analyzed using an Agilent Technologies 2100 Bioanalyzer. The expression levels and identification of alternatively spliced transcripts were determined by aligning the RNA-Seq reads to the mouse genome using HISAT2. Upon read mapping, transcript assembly was executed using String Tie (version 2.1.0)[13], yielding expression profile values for known transcripts in each sample. These values, including read count, FPKM (Fragments per Kilobase of transcript per Million mapped reads), and TPM (Transcripts Per Kilobase Million), were organized based on transcripts/genes. Differential expression analysis was performed using DESeq2, with significance defined as FDR-adjusted p-value < 0.05 and absolute log₂ Fold Change (log₂FC) ≥ 1 in the rSmeg-MIF-IL7 group compared to the control group. Hierarchical clustering analysis was employed to visualize the expression patterns of significant genes in each sample, facilitating the grouping of samples and genes based on the similarity of their expression profiles. This method aids in the visualization of sample and gene clustering, providing insights into their expression patterns.

2.7. Enrichment analysis of DEGs

DAVID Functional Annotation Bioinformatics Microarray Analysis [14] is a free online bioinformatics resource developed by the Laboratory of Human Retrovirology and Immunoinformatics. Gene Ontology (GO) enrichment[15] enables gene annotation and analysis of their respective biological roles. To elucidate the biological function of DEGs, “DAVID” were used to perform GO enrichment analyses.

2.8. Calculation of cell fraction Abundance of Immune Cells

CIBERSORT X is deconvolution tool used to estimate cell type fractions in bulk RNA-seq data from whole blood. The 22 cell types inferred by CIBERSORT X include macrophages, dendritic cells, B cells, T cells, natural killer cells, and other types of immune cells. we used LM22 gene profile of CIBERSORT X to analyze our bulk RNA-seq data. CIBERSORT X digital cytometry cell fraction imputation was performed to implement this analysis, and the algorithm used the default signature matrix to run in 500 permutations without batch corrections.

2.9. Kaplan–Meier plotter database analysis

The Kaplan–Meier plotter (<http://kmplot.com/analysis/>) allows visualization of Kaplan–Meier survival curves based on data from GEO, the European Genome-Phenome Archive, and The Cancer Gene Atlas (TCGA) [16]. In this present study, Tumor patients were divided into high-expression and low-expression groups based on median values of mRNA expression, and the prognostic value of the selected genes in the Bladder Urothelial Carcinoma data set (TCGA, Bladder Cancer) from 405 cases was evaluated[17].

2.10. cBioPortal for Cancer Genomics database analysis

The cBioPortal for Cancer Genomics (<http://www.cbioportal.org/>) serves as an openly accessible platform for interactively exploring multidimensional datasets related to cancer genomics[18]. The genetic alterations in multiple cancers were examined using cBioPortal for Cancer Genomics [19]. In our investigation, we utilized the cBioPortal to examine gene expression patterns and clinical outcomes within the Bladder Urothelial Carcinoma dataset (TCGA, Firehose Legacy), encompassing 413 cases. Through the portal, we accessed Overall Survival Kaplan-Meier Estimates

and disease-free survival data, with associated log rank p-values when available. For our analysis, tumor patients were stratified into high-expression and low-expression groups based on mRNA expression values exceeding or falling below the 30th percentile. Subsequently, we generated percentage bar graphs illustrating tumor stage and grade distributions derived from these parameters using the cBioPortal's analytical tools.

2.11. RNA isolation and quantitative real-time-PCR (qPCR)

The extraction of total RNA was performed as per the Trizol reagent protocol (Ambion Life Technologies). To determine concentration and purity, a Nanodrop-2000 spectrophotometer (Thermo Fisher Scientific) was utilized. PCR primer sets, designed to amplify transcripts of 16 ORFs, ranged from 20 to 25 nucleotides, producing amplicons between 101 and 665 bp. For reverse transcription quantitative PCR (RT-qPCR), 1 μ g of total RNA underwent reverse transcription to complementary DNA using PrimeScript RT Master Mix (Takara, RR036A). Quantitative RT-PCR analysis employed GoTaq SYBR Green PCR Master Mix (Promega, A6001) and was executed on a QuantStudio 3 Real-Time PCR Instrument (Applied BioSystems, A28132). Reaction conditions included initial activation of GoTaq DNA polymerase at 95°C for 2 minutes, followed by 40 cycles of denaturation at 95°C for 15 seconds, annealing/extension at 60°C for 1 minute, and cooling to 4°C. Gene expressions of GAPDH and differentially expressed genes (DEGs) were assessed. DEG expression levels were normalized utilizing the comparative $2^{-\Delta\Delta Ct}$ method for relative quantification.

2.12. Statistical analysis

PRISM software version 9.00 (GraphPad Software, Inc.) was used for statistical analysis, plotting the data, and creating graphs. Two-way ANOVA test and log rank test was done for statistical analysis. Differences were considered statistically significant if $p < 0.05$ *; $p < 0.01$ **; $p < 0.001$ ***. Results are expressed as the mean \pm standard error of mean.

3. RESULTS

3.1. rSmeg-MIF-IL7 vaccine inhibited tumor progression in a syngeneic mouse model of bladder cancer

The rSmeg-MIF-IL7 vaccine was administered three times to a syngeneic mouse model of bladder cancer, following the tumor protocols and experimental timeline provided, to determine its impact on bladder cancer. For tumor sampling, the rSmeg-MIF-IL7 vaccine was administered a total of 7 times, and the experiment was terminated when the tumor size in one of the control mice approached 2000mm³. For the RNA-sequencing, the rSmeg-MIF-IL7 was administered a total of 11 times, and tumor sizes were measured between the control and rSmeg-MIF-IL7 groups up to 24 days and repeated twice (Figure 2A). In all three sets, the rSmeg-MIF-IL7 group showed a significant inhibition of tumor growth compared to the control group (Figure 2B). According to the tumor volume measurements from day 6 to day 15, differences in tumor size began to appear between the control and rSmeg-MIF-IL7 groups from day 10 onwards, with differences exceeding 1100 mm³ after day 15 (Figure 2C). The survival rate of mice in the rSmeg-MIF-IL7 group maintained survival for all mice until the end of the experiment on day 25. In contrast, due to accelerated tumor growth rates after day 13 in the control group, most mice were euthanized after day 15 (Figure 2D). Considering the decrease of tumor volume over time and the survival curve of mice, rSmeg-MIF-IL7 treatment inhibited tumor growth in the bladder cancer mouse model.

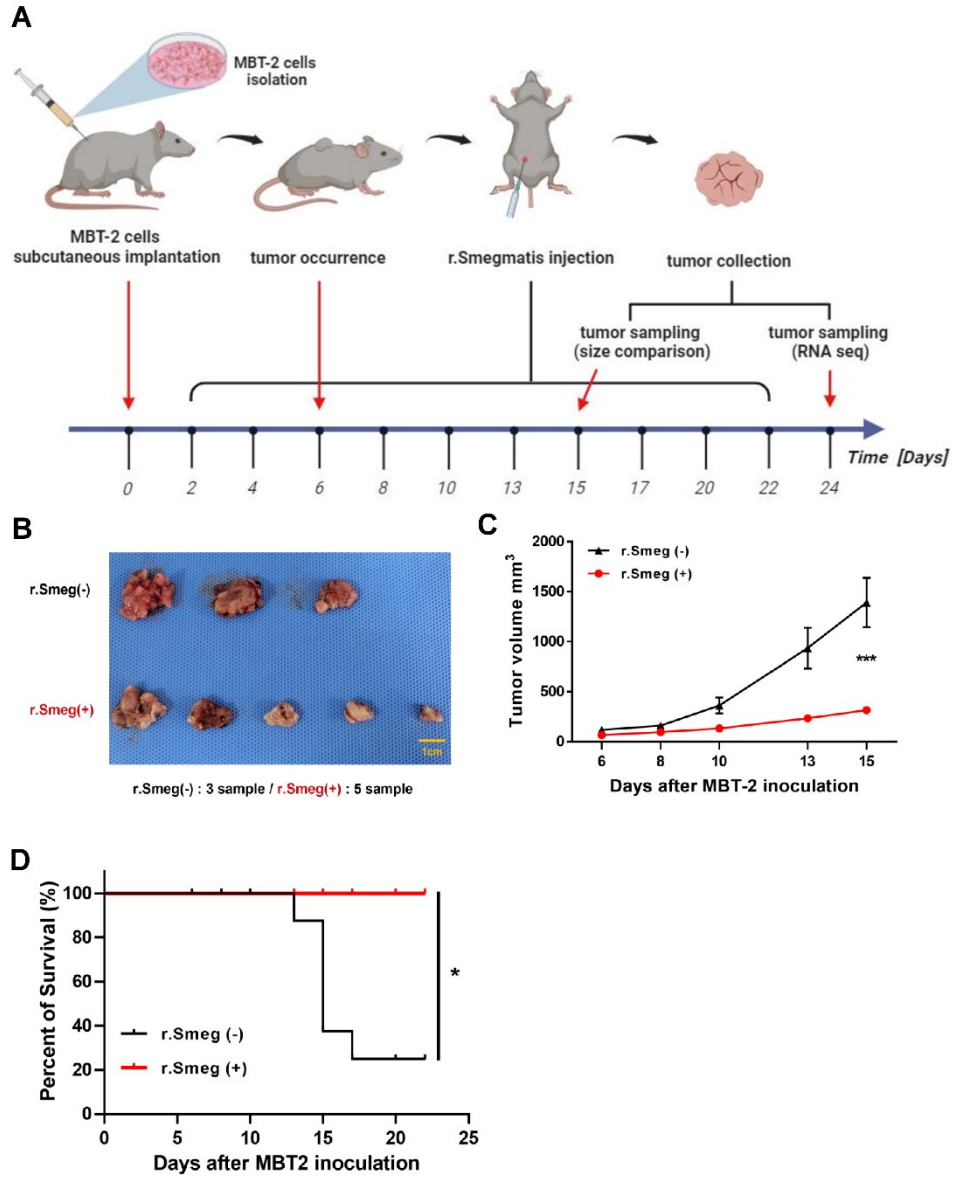


Figure 2. Tumor volume measurements and survival analysis of rSmeg-MIF-IL7 immunization test in the MBT-2 syngeneic subcutaneous tumor mice.

(A) MBT-2 syngeneic subcutaneous tumor mice modeling process and all of experiment experimental timeline. (B) The image showed the tumors dissected from the MBT-2 syngeneic subcutaneous tumor mice group treated with rSmeg-MIF-IL7 vaccine and untreated mice group. (C)

Tumor growth curve was obtained by measuring the volumes of the tumors in the MBT-2 syngeneic subcutaneous tumor mice. Tumor volumes in rSmeg-hMIF-hIL-7 treated group were significantly smaller than control group ($***p \leq 0.001$) on day 15. (D) Survival curve displayed significantly different value between two groups on day 24 ($*p \leq 0.05$). Survival experiment was terminated on day 24.

3.2. DEGs between two groups in primary tumor cells are associated with immune response pathway and negative regulation of angiogenesis

We analyzed three samples of rSmeg-MIF-IL7, which had been observed for tumor growth over 24 days, and four control samples. Using the DESeq2 algorithm, we compared the DEGs between the two groups, which were visualized by the heat map of two-way Hierarchical Clustering (Figure 3A). A total of 398 DEGs were identified, including 256 upregulated and 142 downregulated genes ($\log FC > 1$, $p < 0.05$) (Figure 3B). A volcano plot (Figure 3C) was constructed to visualize the \log_2 of the enrichment ratio alongside the negative logarithm (base 10) of the raw p-values. Mouse DEGs were converted one-to-one to human orthologs of DEGs, total 248 genes, for the purpose of focusing on patient treatment using the Ensembl BioMart data mining tool (<https://asia.ensembl.org>) (Figure 3D). To gain insight into the biological functions of these human orthologs of DEGs, we performed functional annotation analysis of the Differentially Expressed Genes (DEGs) utilizing the DAVID bioinformatics tool (v6.8 online server). Enrichment significance was determined by considering modified Fisher exact p-values ≤ 0.05 and False Discovery Rate (FDR) < 0.05 as strongly enriched. We found that the top 20 Gene Ontology (GO) terms of upregulated and downregulated DEGs by analyzing Biological Process. GO terms of upregulated DEGs indicated that these genes could be categorized into apoptotic process and immune response, including inflammatory response, neutrophil chemotaxis (Figure 3E). This is suggested that rSmeg-MIF-IL7 inhibited abnormal growth of cancer cells through acute inflammatory and immune responses leading to apoptosis [20]. Downregulated DEGs by analyzing Biological Process were enriched in angiogenesis, cell adhesion, immune response, vasculogenesis (Figure 3F). Given that the downregulated genes are associated with terms known to promote tumor growth, rSmeg-MIF-IL7 is suspected to play a crucial biological role in inhibiting tumor growth (Table 1).

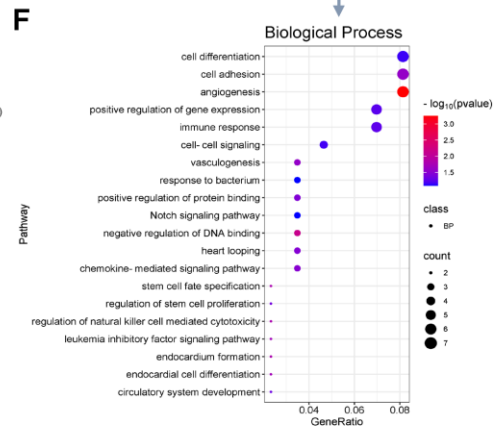
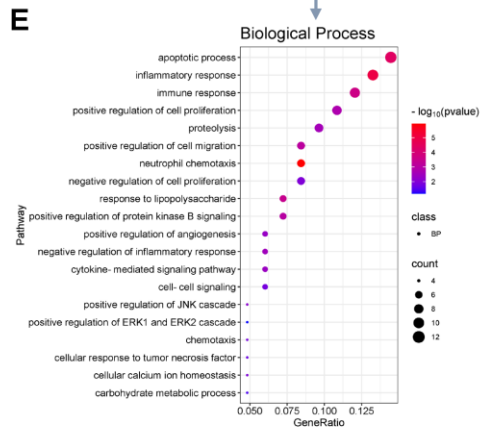
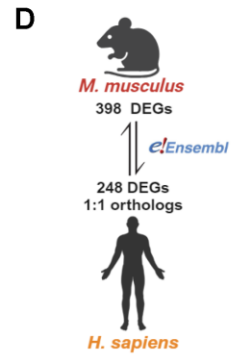
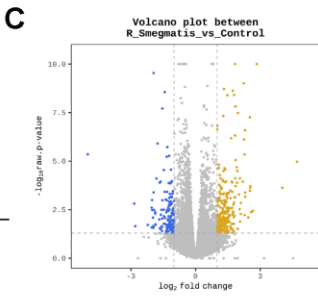
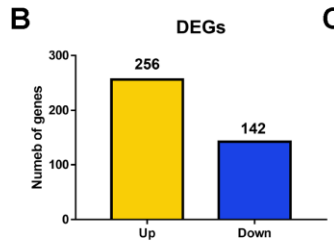
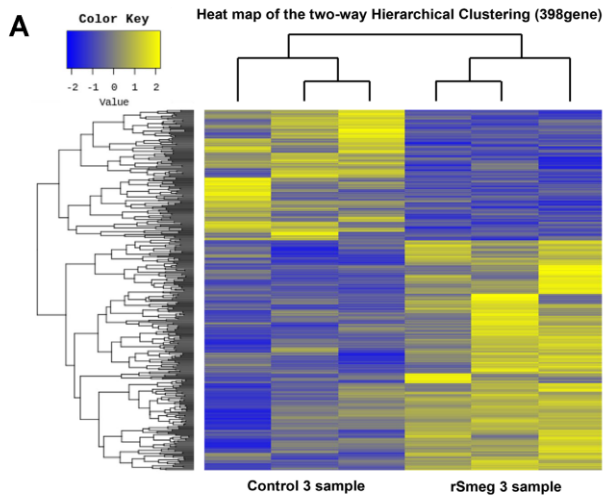


Figure 3. Gene expression overview in rSmeg-MIF-IL7 treated group compared to the control group

(A) Heat map of the Hierarchical Clustering 398 DEGs between the control group and the rSmeg-MIF-IL7 group. The color scale at the left of the heatmap shows the Z-score for normalized value ranging from yellow (High expression) to blue (low expression). (B) The number of the upregulated and downregulated DEGs. (C) Volcano map generated DEGs in rSmeg-MIF-IL7 treated group compared to the control group. Yellow nodes on the left denote upregulated DEGs, while blue nodes on the right represent downregulated DEGs. Gray nodes indicate genes with a p-value of ≤ 0.05 , the red nodes represent significant genes. (E) Top 20 Gene Ontology Biological Process (GOBP) of the upregulated DEGs and (F) top 20 GOBP the downregulated DEGs in rSmeg-MIF-IL7 treated group compared to the control group. In the visualization, the color of each dot corresponds to the p-value, while the size of the dot correlates with the number of genes enriched.

Table 1. Representative significantly enriched pathways of top20 gene ontology biological process and related DEGs

GO Term	Gene Names	Number of Genes	P-value
Over-expressed in r.Smegmatis treated relative to control			
Immune response	IL1A, CCL23, CLEC4D, IL1B, IL1R2, CXCR2, IL7R, SMAD6, THBS1, CCL15	10	2.26E-04
Carbohydrate metabolic process	CHIA, MGAM, ST3GAL5, PYGL	4	0.0374
Under-expressed in r.Smegmatis treated relative to control			
Angiogenesis	ESM1, SOX17, HEY1, SOX18, ANGPTL6, APLNR, VASH1	7	5.57E-04
cell adhesion	VTN, CLCA2, PCDH12, HAPLN4, CD33, SIGLEC6, PCDHGA9	7	0.026167
cell differentiation	SPIB, FGF17, SOX17, SOX18, ANGPTL6, TLL1, ZNF423	7	0.04054994
positive regulation of protein binding	SPTA1, VTN, ADD2	3	0.03557

3.3. CD8+, CD4+ memory T cells activated, abundance in rSmeg-MIF-IL7 group

Gene expression data from both the control and rSmeg-MIF-IL7 groups underwent analysis to quantify immune cell infiltration levels using CIBERSORTx, an analytical tool with predefined gene signatures for 22 distinct immune cell types (Figure 4Aa). Among these 22 cell types, four, including CD8+ T cells and activated CD4+ memory T cells, exhibited significant differences in proportions between the rSmeg-hMIF-hIL-7 and control groups. Specifically, CD8+ T cells displayed a 0.05 increase (Figure 4Ab), while activated CD4+ memory T cells showed a 0.02 increase (Figure 4Ac) in proportion within the rSmeg-MIF-IL7 group compared to the control group.

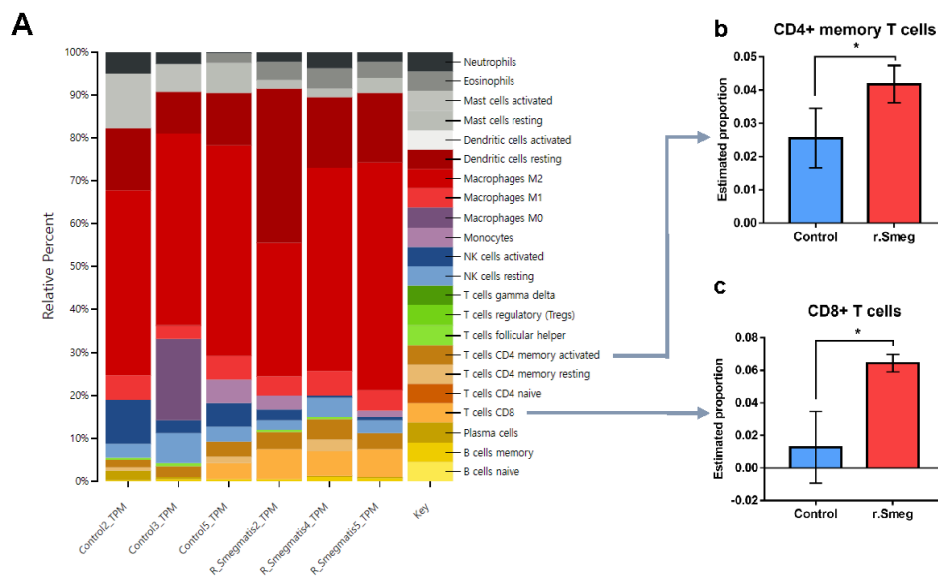


Figure 4. immune cells infiltration generated using CIBERSORTx

(A) (a) The relative percentage of 22 immune cell types were deconvoluted from the RNA-seq data. Estimated proportion of the abundance of (b) CD8+ T cells, (c) CD4+ memory T cells in rSmeg-MIF-IL7 treated group compared to the control group ($*p \leq 0.05$).

3.4. Prognostic diagnostic markers screening in TCGA Bladder Urothelial Carcinoma study

To assess the potential applicability of the rSmeg-MIF-IL7 vaccine in bladder cancer patients, a prognostic gene screening analysis was conducted using the TCGA-BLCA dataset. Among all 403 bladder cancer patients, the deceased group (n=180) and living group (n=228) were separated based on survival status. Compared to previous experiments, the deceased group was designated as the control group, and the living group as the treatment group (Figure 5A). A total of 758 DEGs satisfying $FC > 1.5$, $p < 0.05$ were identified. Among the human orthologs of DEGs in the mouse (248 genes) and the TCGA dataset DEGs (758 genes), 23 genes with overlapping gene expression patterns were found (Figure 5B). In the patient survival analysis with the KM plotter, after filtering the 23 genes, 9 genes associated with good prognosis in bladder cancer patients were selected. High expression of CCL15 ($p = 2.7e-05$, HR = 1.85), CCRL2 ($p = 0.00016$, HR = 2), SMAD6 ($p = 5.5e-05$, HR = 1.85), ST3GAL5 ($p = 0.00056$, HR = 2), and SGK2 ($p = 0.00029$, HR = 1.75) significantly increased the median overall survival (OS) in bladder cancer. Conversely, high expression of ABCA4 ($p = 2.7e-05$, HR = 1.85), ADD2 ($p = 0.0012$, HR = 0.69), SIGLEC6 ($p = 5.5e-05$, HR = 1.85), and TLL1 ($p = 0.00056$, HR = 0.5) showed better outcomes and survival in bladder cancer patients (Figure 5C). In the TCGA-BLCA dataset, the gene expression of the selected 9 genes in the deceased group compared to the living group showed upregulation in CCL15, CCRL2, SMAD6, ST3GAL5, and SGK2, while downregulation was observed in ABCA4, ADD2, SIGLEC6, and TLL1 (Figure 5D). These gene expression patterns align with the mouse gene expression patterns of rSmeg-MIF-IL7 from RNA sequencing (Figure 5E). To determine the association of the selected 9 genes with the top 20 GO Biological Process terms and genes related to CD4+ memory T cells activated and CD8+ T cells found through Amigo2, STRING interaction network tool (<https://string-db.org>) was utilized. Interaction with CD4+ memory T cells activated was confirmed in CCL15, CCRL2, SMAD6, SGK2, and TLL1 (Figure 5Fa). Interaction with CD8+ T cells was confirmed in CCL15, CCRL2, SMAD6, ST3GAL5 (Figure 5Fb). Through Venn diagrams between the top 20 GO terms Biological Process-related genes (total 71 genes) and the selected 9 genes, overlapping genes CCL15, SMAD6, ST3GAL5, ADD2, and SIGLEC6 were identified (Figure 5Fc). Through the aforementioned three analyses, a total of 8 significant genes, CCL15, CCRL2, SMAD6, ST3GAL5, SGK2, ADD2, SIGLEC6, and TLL1, were identified. These genes are believed to

influence the survival of bladder cancer patients and can serve as diagnostic markers to distinguish bladder cancer patient groups suitable for rSmeg-MIF-IL7 vaccine therapy.

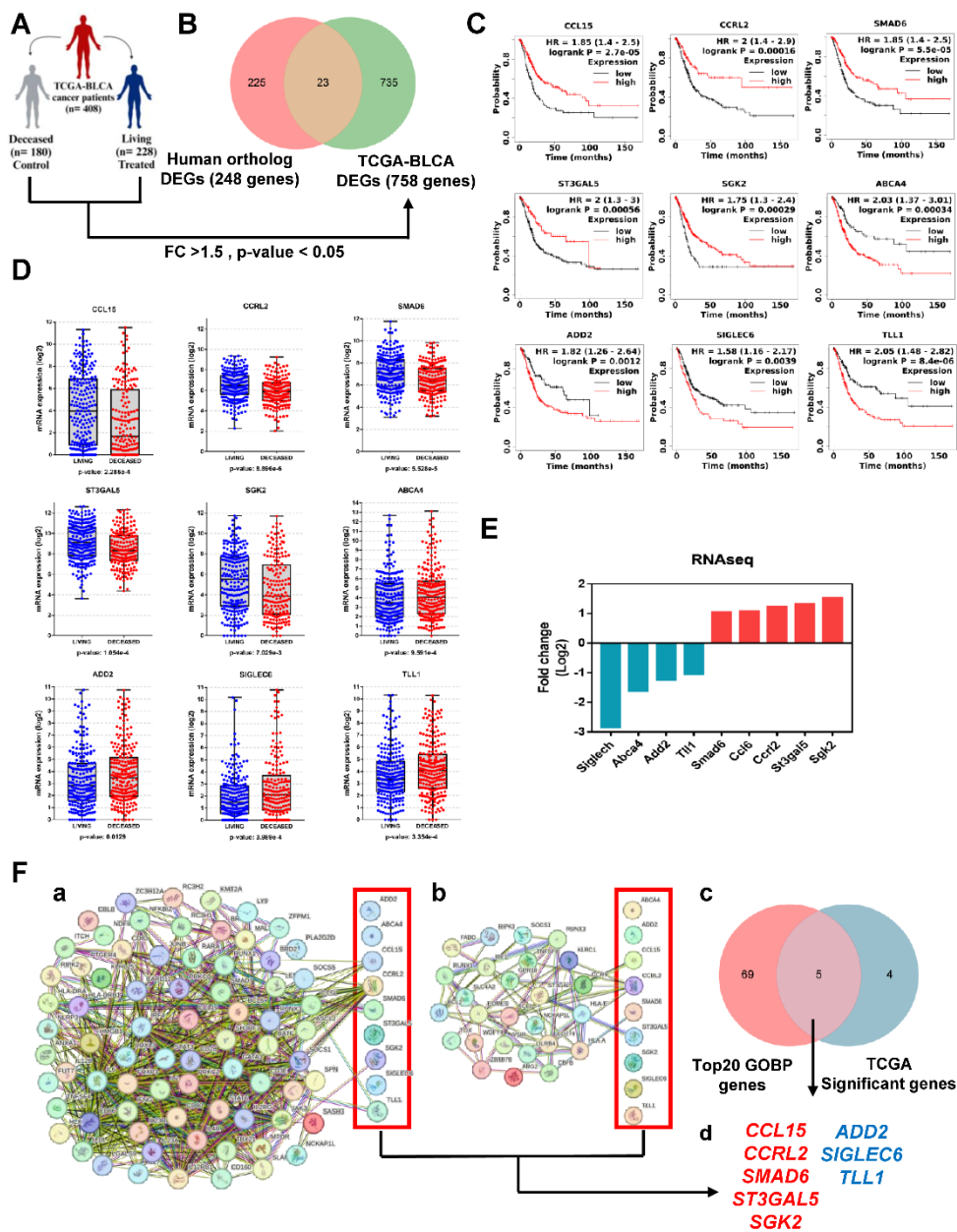


Figure 5. diagnosis markers selection by using TCGA bladder cancer (TCGA-BLCA) clinic data set and KM-plotter

(A) Schematic of group design to TCGA bladder cancer patients. DEG extraction in the Living group (n = 228) compared to the Deceased group (n = 180) ($\log FC > 1, p \leq 0.05$). (B) Venn diagram presentation of the intersection of genes between human orthologs of DEGs (248 genes) and DEGs of TCGA-BLCA (758 genes) in the living group compared to the deceased group. (C) Survival analysis of bladder cancer patient groups with high (red) and low (black) expression of 9 genes (CCL15, CCRL2, SMAD6, ST3GAL5, SGK2, ABCA4, ADD2, SIGLEC6, TLL1). The survival curves plotted using KM plotter. The hazard ratio (HR) and log-rank p -value are in each figure ($p \leq 0.05$). (D) mRNA expression of 9 genes (CCL15, CCRL2, SMAD6, ST3GAL5, SGK2, ABCA4, ADD2, SIGLEC6, TLL1) in the Living group and the Deceased group. (E) The fold changes of 9 mouse DEGs (Ccl6, Ccl2, Smad6, St3gal5, Sgk2, Abca4, Add2, Siglech, Tll1) in rSmeg-hMIF-hIL-7 treated group compared to the control group. (F) Genes related (a) CD4⁺ memory T cells activated, (b) CD8⁺ T cells presented networks interaction with 9 genes (CCL15, CCRL2, SMAD6, ST3GAL5, SGK2, ABCA4, ADD2, SIGLEC6, TLL1) using STRING tool. (c) Venn diagram presentation of the intersection of genes between genes related top 20 GOBP and prognostic significant 9 genes. (d) selected 8 genes.

3.5. Differences in Neoplasm stage and grade based on gene expression levels in patients

The indicators of tumors are known to be determined by two factors: the metastatic staging of the tumor and the histologic tumor grade score. To verify whether the expression differences of the 8 diagnostic markers are indeed different in bladder cancer patients' tumor stage and tumor grade, we divided the TCGA-BLCA (Bladder Cancer) patient group based on gene expression levels for comparison. The upper quartile, defined as the top 30% of individuals with high gene expression, was labeled as Q1, while the lower quartile, defined as the bottom 30% with low gene expression, was labeled as Q2. Patient classification based on gene expression levels and the analysis of tumor stage and grade were investigated using cBioportal. CCL15, CCRL2, SMAD6, and ST3GAL5 showed lower malignancy in the Q1 group, whereas ADD2 and TLL1 showed lower malignancy in the Q2 group (Figure 6Aa-d, f, h). SIGLEC6 exhibited expression differences based on grade, but no significance was observed based on stage (Figure 6Ag). SGK2 did not show significance in either stage or grade (Figure 6Ae). While the SGK2 expression difference was related to the patients' survival probability, it was not associated with the malignancy of the tumor.

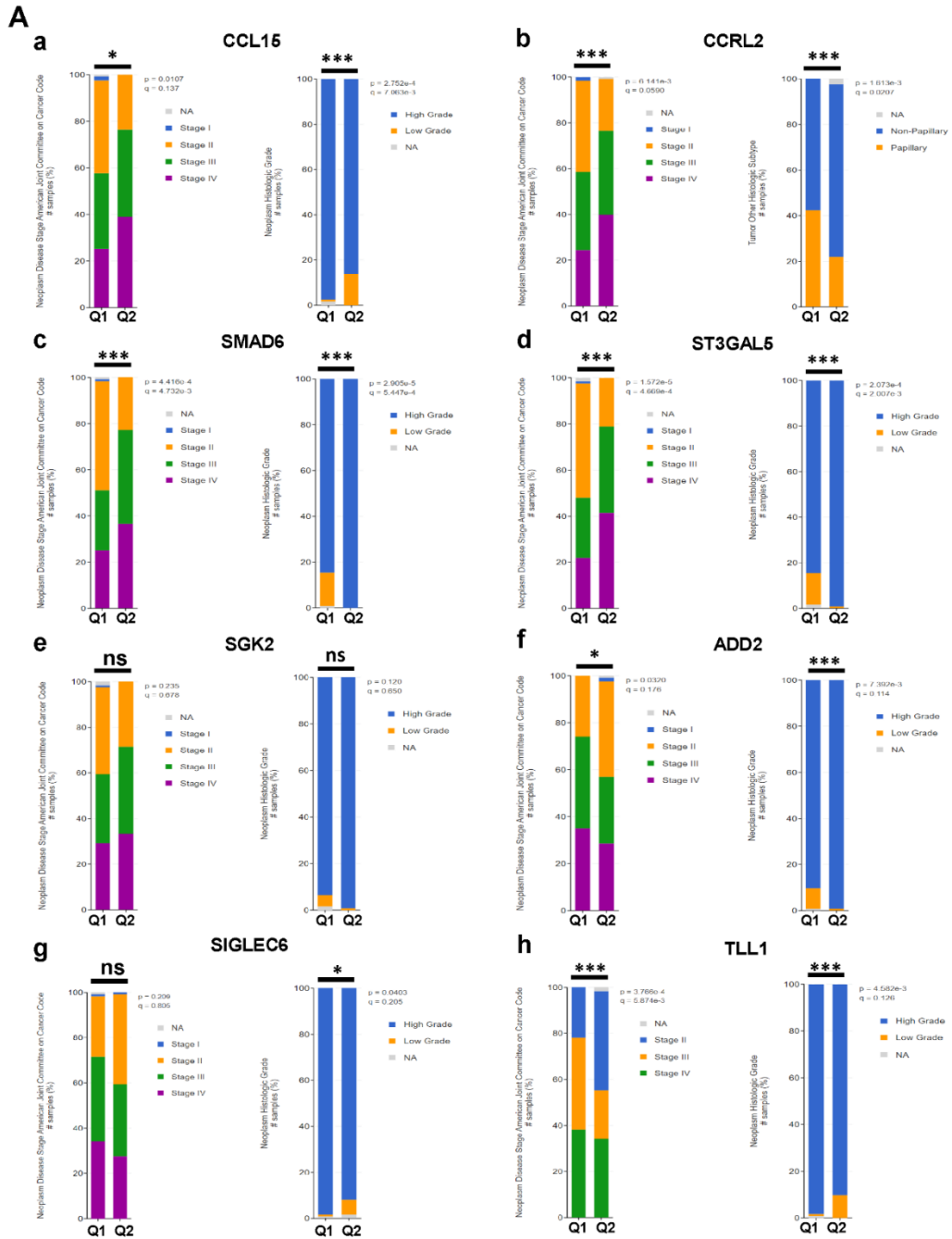


Figure 6. Summary of neoplasm stage and histologic grade based on gene expression in bladder cancer patients

(A) Neoplasm stage and histologic grade based on expression of 8 genes. Neoplasm stage is left graph and histologic grade is right. (a) CCL15, (b) CCRL2, (c) SMAD6, (d) ST3GAL5, (e) SGK2, (f) ADD2, (g) SIGLEC6, (h) TLL1 ($*p \leq 0.05$, $***p \leq 0.001$)

3.6. Validation of diagnostic marker expression at both mRNA and protein level in bladder cancer

8 genes have been selected as diagnostic markers to determine the suitability of rSmeg-MIF-IL7 vaccine treatment for bladder cancer patients clinically. These genes were validated against mouse mRNA-seq results using qRT-PCR to compare mRNA expression levels. Protein expression levels were validated using data from The Human Protein Atlas (<https://www.proteinatlas.org>). At the mRNA level, all eight genes showed consistent expression differences with the RNA-Seq data, validating their efficacy (Figure 7A). A representative IHC image showed that CCRL2 and SGK2 staining was low in bladder carcinoma tissues, while ADD2 and SIGLEC6 staining was high in bladder carcinoma tissues. Since CCRL2 and SGK2 are upregulated at the mRNA level, rSmeg-MIF-IL7 treatment is suitable for bladder cancer patient groups with low protein expression. On the other hand, since ADD2 and SIGLEC6 are downregulated at the mRNA level, rSmeg-MIF-IL7 vaccine treatment is suitable for bladder cancer patient groups with high protein expression (Figure 7B). The IHC images for CCL15, SMAD6, ST3GAL5, and TLL1 could not be validated due to insufficient data in The Human Protein Atlas.

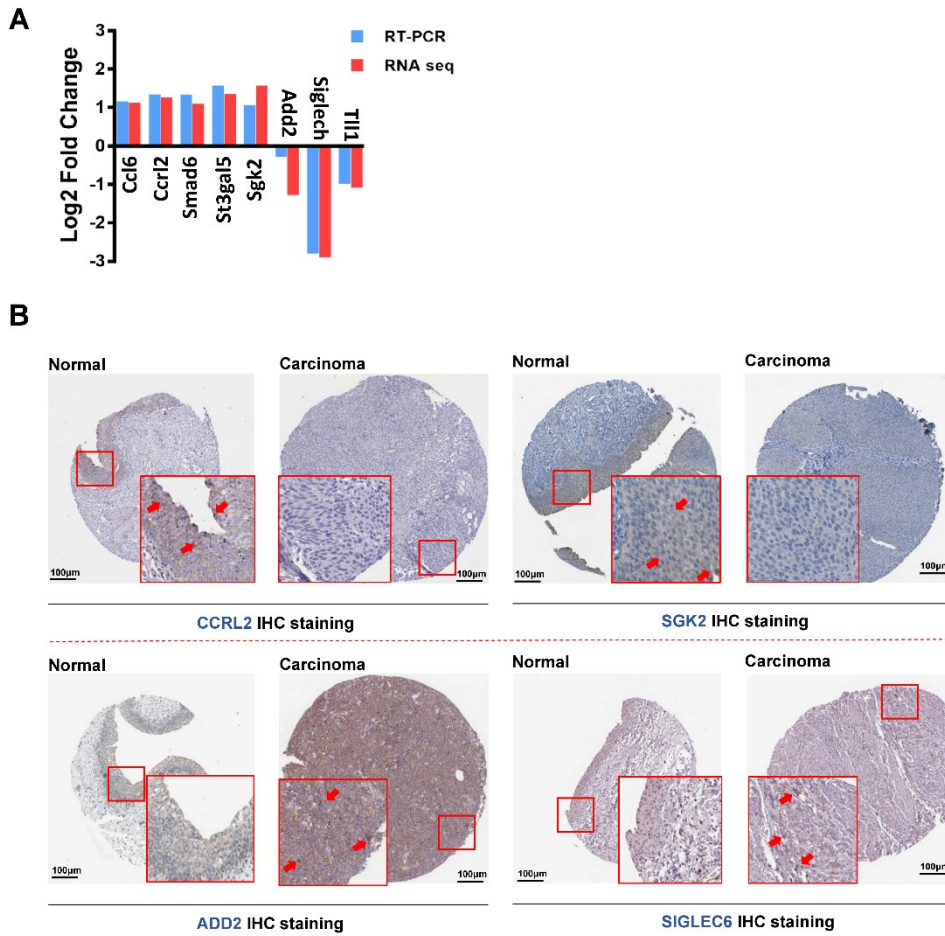


Figure 7. validation of Diagnosis markers by QRT-PCR results and Immunohistochemistry staining image

(A) Validation of RNA-seq results of gene expression using real-time PCR analysis. Coherence of the expression pattern for 8 genes was presented in RNA-seq and real-time PCR. The relative transcript levels were shown as Log2 fold change. (B) The immunohistochemistry staining based on the Human Protein Atlas database (HPAD). Protein expression levels of CCRL2, SGK2, ADD2, SIGLEC6 in bladder carcinoma and bladder normal tissues.

4. DISCUSSION

The objective of this study was to investigate whether the fusion protein rSmeg-MIF-IL7, which expresses a combination of h-MIF promoting cancer and inflammatory responses, promotes T-cell differentiation, and induces CTL responses, could inhibit tumor growth in a mouse bladder cancer model and be applicable to patients. The development of the rSmeg-MIF-IL7 vaccine, designed to replace BCG therapy, is significant as the first application to a bladder cancer mouse model. Additionally, from a tumor growth inhibition perspective, the results align with previous research showing that the rSmeg-MIF-IL7 vaccine enhanced anti-MIF immunity by inhibiting the MIF signaling pathway in a colon adenocarcinoma model [10]. While it is known that hMIF delivered by the shuttle vector rSmeg-MIF-IL7 binds to CD74 and CD44 and proceeds through the PI3K/Akt signaling pathway [21], our mouse mRNA-seq results did not show differential expression of the CD74 and CD44 genes. This suggests that tumor growth inhibition in the bladder cancer model may not simply result from reduced MIF expression. The mRNA-seq results from mice showed overexpression of IL-7R in the rSmeg-MIF-IL7 group. This indicates the possibility that IL-7 was induced by the rSmeg-MIF-IL7 vaccine, given the increased IL-7 receptor expression. So, we gave attention to the immune-enhancing function of IL-7, which promotes T-cell differentiation and induces CTL responses. The encoding protein of the mouse ortholog gene for Human C-C chemokine ligand 15 (CCL15), known as C-C chemokine ligand 6 (CCL6), has been associated with the enhancement of memory CD8⁺ T cell differentiation, correlating with an increase in CD4⁺ memory T and CD8⁺ memory T cells [22, 23]. Siglec-H, a member of the sialic acid binding Ig-like lectin (Siglec) family, has recently been identified as a specific surface marker for plasmacytoid dendritic cells (pDCs) in mice [24]. pDCs can present antigens not only to CD4⁺ T cells but also cross-present antigens to CD8⁺ T cells. Mediated antigen presentation has been reported to promote CD4⁺ regulatory T cells (Tregs), reducing the responsiveness of CD4⁺ and CD8⁺ T cells. Elevated expression of Ccl6 due to increased IL-7 expression values in infected mice by rSmeg-MIF-IL7 and decreased expression values of Siglec-H are shown to induce enhanced CTL (Cytotoxic T Lymphocytes) in CD4⁺ and CD8⁺ T cells. In a similar context, research has reported that the human ortholog gene of Siglec-H, Siglec6, is upregulated in bladder cancer patients, correlating with unfavorable tumor outcomes and patient survival [25]. Beyond immune cell response, enrichment

analysis further clarified that rSmeg-MIF-IL7 is associated with other biological processes that inhibit cancer growth.

However, the relative gene ratio for inflammatory response was higher in the rSmeg-MIF-IL7 group. While inflammation plays a crucial role in tissue repair or regeneration against pathogens in host defense, it is mostly known to promote cancer by signaling tumor-promoting functions in cancer cells [26]. However, it cannot be concluded that inflammation always serves as a tumor-promoting signal without considering the functions of immune cells and acute responses. ST3GAL5 is a protein that catalyzes the formation of Ganglioside GM3 in the Carbohydrate metabolic process [27]. Elevated levels of ST3GAL5 are known in various cancer types and can be utilized as tumor-associated carbohydrate antigens [28]. ST3GAL5, which catalyzes GM3 known to inhibit tumor cell proliferation through angiogenesis suppression or reduced cell motility, may demonstrate anti-tumor effects in human bladder cancer [29-31]. In one study, it was reported that the biased expression of M2 macrophages due to decreased ST3GAL5 expression affects microvascular formation, pathological outcomes, tumor grade, and invasion in bladder cancer, although the exact mechanism remains largely unknown. The Adducin family members, ADD1 and ADD3, are known to be upregulated in various cancer types. They are believed to inhibit the transcription of the p53 gene, thereby promoting cell differentiation, migration, and invasion in tumor cells[32], contributing to tumor metastasis. However, ADD2 is known as a crucial gene for the formation and stabilization of the membrane-cytoskeleton and is only recognized for its importance in cell movement and adhesion. Its role in tumors remains unknown. While various genes seem to influence the anti-cancer mechanism of rSmeg-MIF-IL7, some results contradict known anti-cancer mechanisms, suggesting the need for further experiments to clarify the exact mechanism. Furthermore, through bioinformatics analysis, we confirmed how selected diagnostic markers identified in the rSmeg-MIF-IL7 group correlate with the prognosis of actual bladder cancer patients. This suggests that these markers could be utilized for observing malignant prognoses in clinical studies and potentially grouping patients showing opposite trends in gene expression to select those who might exhibit optimal efficiency. There are, of course, limitations as well. The therapeutic efficacy of rSmeg-MIF-IL7 vaccine has not been verified in an orthotopic mouse model, which closely mimics human bladder cancer, nor has a comparison with BCG been conducted in this study. In future research, we aim to conduct comparative studies between rSmeg-MIF-IL7 and BCG in an orthotopic mouse model of bladder cancer. Additionally, although the anti-cancer mechanisms of the selected

diagnostic markers have not been clearly elucidated, making them unreliable markers, there is value in further researching the use of rSmeg-MIF-IL7 vaccine in patients, considering our comparative analysis of mouse experimental results and patient data. Thus, the rSmeg-MIF-IL7 vaccine has shown potential as a therapeutic agent for bladder cancer, and the limitations of this study will be addressed in future research endeavors.

5. CONCLUSION

In conclusion, the rSmeg-MIF-IL7 vaccine induced immune infiltration of CD4⁺ and CD8⁺ T cells at the tumor site in mice and demonstrated tumor suppression through the expression of genes such as CCL6 and SIGLEC-H. Through various analyses to select genes applicable to actual patients, eight genes including CCL15 and SIGLEC6 were classified as disease markers. It is believed that these genes, based on their expression differences leading to patient grouping, can serve as indicators for determining the target for treatment with rSmeg-MIF-IL7.

REFERENCES

1. Malmstrom, P.U., et al., *Five-year followup of a prospective trial of radical cystectomy and neoadjuvant chemotherapy: Nordic Cystectomy Trial I. The Nordic Cooperative Bladder Cancer Study Group.* J Urol, 1996. **155**(6): p. 1903-6.
2. Alexandroff, A.B., A.M. Jackson, M.A. O'Donnell, and K. James, *BCG immunotherapy of bladder cancer: 20 years on.* Lancet, 1999. **353**(9165): p. 1689-94.
3. Batista, R., et al., *Validation of a Novel, Sensitive, and Specific Urine-Based Test for Recurrence Surveillance of Patients With Non-Muscle-Invasive Bladder Cancer in a Comprehensive Multicenter Study.* Front Genet, 2019. **10**: p. 1237.
4. Guallar-Garrido, S. and E. Julian, *Bacillus Calmette-Guerin (BCG) Therapy for Bladder Cancer: An Update.* Immunotargets Ther, 2020. **9**: p. 1-11.
5. Cernuschi, T., S. Malvolti, E. Nickels, and M. Friede, *Bacillus Calmette-Guerin (BCG) vaccine: A global assessment of demand and supply balance.* Vaccine, 2018. **36**(4): p. 498-506.
6. Choi, Y., et al., *Gemcitabine and Docetaxel Combination for Advanced Soft Tissue Sarcoma: A Nationwide Retrospective Study.* Cancer Res Treat, 2018. **50**(1): p. 175-182.
7. Waldman, A.D., J.M. Fritz, and M.J. Lenardo, *A guide to cancer immunotherapy: from T cell basic science to clinical practice.* Nat Rev Immunol, 2020. **20**(11): p. 651-668.
8. Lee, H., et al., *The development of a novel Mycobacterium-Escherichia coli shuttle vector system using pMyong2, a linear plasmid from Mycobacterium yongonense DSM 45126T.* PLoS One, 2015. **10**(3): p. e0122897.
9. Kim, B.J., et al., *Recombinant Mycobacterium smegmatis with a pMyong2 vector expressing Human Immunodeficiency Virus Type I Gag can induce enhanced virus-specific immune responses.* Sci Rep, 2017. **7**: p. 44776.
10. Jeong, H., S.Y. Lee, H. Seo, and B.J. Kim, *Recombinant Mycobacterium smegmatis delivering a fusion protein of human macrophage migration inhibitory factor (MIF) and IL-7 exerts an anticancer effect by inducing an immune response against MIF in a tumor-bearing mouse model.* J Immunother Cancer, 2021. **9**(8).

11. Grieb, G., M. Merk, J. Bernhagen, and R. Bucala, *Macrophage migration inhibitory factor (MIF): a promising biomarker*. Drug News Perspect, 2010. **23**(4): p. 257-64.
12. Sheikh, A., et al., *Selective dependence on IL-7 for antigen-specific CD8 T cell responses during airway influenza infection*. Sci Rep, 2022. **12**(1): p. 135.
13. Pertea, M., et al., *Transcript-level expression analysis of RNA-seq experiments with HISAT, StringTie and Ballgown*. Nat Protoc, 2016. **11**(9): p. 1650-67.
14. Sherman, B.T., et al., *DAVID: a web server for functional enrichment analysis and functional annotation of gene lists (2021 update)*. Nucleic Acids Res, 2022. **50**(W1): p. W216-W221.
15. The Gene Ontology, C., *Expansion of the Gene Ontology knowledgebase and resources*. Nucleic Acids Res, 2017. **45**(D1): p. D331-D338.
16. Cooper, L.A., et al., *PanCancer insights from The Cancer Genome Atlas: the pathologist's perspective*. J Pathol, 2018. **244**(5): p. 512-524.
17. Cancer Genome Atlas Research, N., *Comprehensive molecular characterization of urothelial bladder carcinoma*. Nature, 2014. **507**(7492): p. 315-22.
18. Deng, M., J. Bragelmann, J.L. Schultze, and S. Perner, *Web-TCGA: an online platform for integrated analysis of molecular cancer data sets*. BMC Bioinformatics, 2016. **17**: p. 72.
19. Cerami, E., et al., *The cBio cancer genomics portal: an open platform for exploring multidimensional cancer genomics data*. Cancer Discov, 2012. **2**(5): p. 401-4.
20. Pfeffer, C.M. and A.T.K. Singh, *Apoptosis: A Target for Anticancer Therapy*. Int J Mol Sci, 2018. **19**(2).
21. Oliveira, C.S., et al., *Macrophage migration inhibitory factor engages PI3K/Akt signalling and is a prognostic factor in metastatic melanoma*. BMC Cancer, 2014. **14**: p. 630.
22. He, B., et al., *CD8(+) T Cells Utilize Highly Dynamic Enhancer Repertoires and Regulatory Circuitry in Response to Infections*. Immunity, 2016. **45**(6): p. 1341-1354.
23. Wagner, C.A., et al., *Myelin-specific CD8+ T cells exacerbate brain inflammation in CNS autoimmunity*. J Clin Invest, 2020. **130**(1): p. 203-213.

24. Blasius, A.L. and M. Colonna, *Sampling and signaling in plasmacytoid dendritic cells: the potential roles of Siglec-H*. Trends Immunol, 2006. **27**(6): p. 255-60.
25. Benmerzoug, S., et al., *Siglec-6 as a New Potential Immune Checkpoint for Bladder Cancer Patients*. Eur Urol Focus, 2022. **8**(3): p. 748-751.
26. Greten, F.R. and S.I. Grivennikov, *Inflammation and Cancer: Triggers, Mechanisms, and Consequences*. Immunity, 2019. **51**(1): p. 27-41.
27. Berselli, P., et al., *Human GM3 synthase: a new mRNA variant encodes an NH2-terminal extended form of the protein*. Biochim Biophys Acta, 2006. **1759**(7): p. 348-58.
28. Zheng, C., M. Terreni, M. Sollogoub, and Y. Zhang, *Ganglioside GM3 and Its Role in Cancer*. Curr Med Chem, 2019. **26**(16): p. 2933-2947.
29. Satoh, M., et al., *Enhanced GM3 expression, associated with decreased invasiveness, is induced by brefeldin A in bladder cancer cells*. Int J Oncol, 2001. **19**(4): p. 723-31.
30. Wang, H., et al., *Antitumor effects of exogenous ganglioside GM3 on bladder cancer in an orthotopic cancer model*. Urology, 2013. **81**(1): p. 210 e11-5.
31. Kawamura, S., et al., *Glycolipid composition in bladder tumor: a crucial role of GM3 ganglioside in tumor invasion*. Int J Cancer, 2001. **94**(3): p. 343-7.
32. Luo, C. and J. Shen, *Adducin in tumorigenesis and metastasis*. Oncotarget, 2017. **8**(29): p. 48453-48459.

ABSTRACT (IN KOREAN)

방광암 마우스 모델에 재조합 *M. smegmatis*의 검증 및 방광암 임상 데이터 적용을 통한 진단 표지자 발굴

방광암의 치료제인 BCG(Bacillus Calmette-Guérin)는 고위험 NMIBC의 TURBT 이후 MIBC로의 진행을 억제할 수 있는 가장 효과적이고 유일한 치료로 알려져 있다. 하지만, 약 30-45%의 NMIBC 환자가 무반응을, 약 20%의 환자가 부작용을 경험한다. 또한, BCG 생산은 결핵균의 느린 성장 속도와 엄격한 제조과정으로 현재 전세계적인 공급 부족 문제를 겪고 있다. 이전 연구에서 BCG의 대안으로 제시된 rSmeg-MIF-IL7 백신을 항 종양 면역 치료제로서의 가능성을 제시했다. 우리는 마우스 방광암 모델을 만들어 rSmeg-MIF-IL7 백신을 투여를 첫 시도하였고 결과적으로 항 종양 효과와 bioinformatics 분석에서 rSmeg-hMIF-hIL7 그룹에서의 종양 샘플 내에 CD8+, CD4+ memory T cells의 면역 침윤을 확인하였다. 추가로 임상적으로 치료제로써 가능성이 있는지 확인하기 위해 우리의 유전자 발현 분석과 TCGA 데이터 셋의 연관성 분석을 진행했고 유전자 발현에 따른 생존 여부와 악성도를 판별한 결과 rSmeg-MIF-IL7 백신 치료에 적합한 환자 그룹을 판별할 수 있는 diagnostic markers인 CCL15, SIGLEC6 등 8가지의 유전자들을 발굴하였다. 결론적으로, 우리는 rSmeg-MIF-IL7의 마우스 방광암 모델에서의 항종양 효과를 보여주었고 임상적으로 적용할 수 있는 가능성까지 확인할 수 있었다.

핵심 되는 말: 방광암, 재조합 스메그마티스, BCG, 면역 침윤, CCL15, SIGLEC6